

# Investigation of the transverse beam dynamics in the thermal wave model with a functional method

Ji-ho Jang<sup>1</sup>, Yong-sub Cho, Hyeok-jung Kwon

*Korea Atomic Energy Research Institute, Daejeon 305-353, Korea*

## Abstract

We investigate the transverse beam dynamics in the thermal wave model by using a functional method. It can describe the beam optical elements separately with a kernel for a component. The method can be applied to the general quadrupole magnets beyond a thin lens approximation as well as drift spaces. We found that the model can successfully describe the PARMILA simulation result with a laminar input beam.

PACS number(s): 29.27.-a, 29.27.Eg

Key Words: Transverse Beam Dynamics, Thermal Wave Model, Functional Method

arXiv:physics/0608173 v1 17 Aug 2006

---

<sup>1</sup>jangjh@kaeri.re.kr

The thermal wave model is an efficient way to study the beam dynamics of the relativistic charged particles. The Schrödinger-type equation in the model governs the time evolution of the beam wave function whose magnitude squared is proportional to the particle number densities[1]. The model has successfully explained the filamentation of a particle beam and the self-pinching equilibrium in collisionless plasma[2]. It was also used to estimate the luminosity in a linear collider where a spherical aberration was present[3]. The model can also provide some insight on a halo formation by introducing a Gaussian slit[4].

Transverse beam dynamics is another application area of the thermal wave model. In Ref. [5], the authors investigated the beam wave function through a quadrupole magnet with sextupole and octupole perturbations followed by a long drift space under the thin lens approximation. There is also a paper on the phase space behavior of the particle beam in the transverse directions where the Wigner and Husimi functions are used as the phase space distribution functions[6].

In this work, we investigate the transverse beam dynamics in the thermal wave model by using the functional integral method [7]. Since the method can be extended to the lattice structure including general quadrupole magnets beyond a thin lens approximation and it treats the beam optical elements individually, it is possible to systematically analyze a beam motion in each element under a realistic environment such as a FODO lattice. We found that the model can successfully explain the PARMILA[8] simulation results by using a laminar input beam without space charge effects.

In the thermal wave model, the time evolution of the beam wave function for the relativistic charged particles can be described by the Schrödinger-type equation in a transverse direction as follows,

$$i \epsilon \frac{\partial \psi(x, z)}{\partial z} = - \frac{\epsilon^2}{2} \frac{\partial^2}{\partial x^2} \psi(x, z) + U(x, z) \psi(x, z), \quad (1)$$

where  $z = ct$  is the longitudinal distance of the beam movement and  $U(x, z) \equiv u(x, z)/m_0\gamma_r\beta_r^2c^2$  is the dimensionless potential with the relativistic parameters,  $\beta_r = v/c$  and  $\gamma_r = (1 - \beta_r^2)^{1/2}$ .  $\epsilon$  represents the emittance of the input beam. The transverse beam distribution can be obtained by the magnitude squared of the beam wave function,  $\rho(x, z) = N |\psi(x, z)|^2$  with the particle number of  $N$ . In this convention, the beam wave function satisfies the normalization condition as follows,  $\int_{-\infty}^{\infty} |\psi(x, z)|^2 dx = 1$ .

We can solve the differential equation by imposing the following two boundary condition,  $\sigma^2(z=0) = \sigma_0^2$  and  $\frac{1}{\sigma} \frac{d\sigma}{dz} \Big|_{z=0} = \frac{1}{\rho_0}$  [5]. The  $\sigma(z)$  denotes the root mean square (rms) size of the beam distribution and  $\rho(z)$  is the curvature radius of the beam wave function along the beam direction.

Another efficient way to solve the differential equation is known as the functional integral method [7] where the resulting wave function is given by the product of a kernel (or propagator) and the initial beam wave function [5],

$$\psi(x_f, z_f) = \int_{-\infty}^{\infty} dx_i K(x_f, z_f; x_i, z_i) \psi(x_i, z_i). \quad (2)$$

Since a kernel can represent an optical element like a quadrupole magnet or a drift space, the functional method can separate a multi-components problem into several single-component problems. This property is the main advantage of this functional method in the thermal wave model.

We can obtain the kernels from the path integral method directly as follows,

$$K(x_f, z_f; x_i, z_i) = \int \mathcal{D}[x(z)] e^{iS(z)/\epsilon}, \quad (3)$$

where  $S(z) = \int_{z_i}^{z_f} dz \mathcal{L}(x(z), x'(z))$  is called the action. The Lagrangian,  $\mathcal{L}$ , of a system is the difference of the kinetic and potential energy terms.

In this work, we will restrict our attention to a system consisting of quadrupole magnets and drift spaces. The potential energy terms of the beam optical elements are given by

$$V(x) = \begin{cases} 0 & \text{for a drift space,} \\ \frac{1}{2}k_1x^2 & \text{for a quadrupole magnet,} \end{cases} \quad (4)$$

where  $k_1$  is positive in the focusing case. The potential term for the defocusing magnet is  $-(k_1/2)x^2$ .

The kernel,  $K_0$ , for a drift space which has no potential term is given by

$$K_0(x_f, z_f; x_i, z_i) = \left( \frac{1}{2\pi i \epsilon (z_f - z_i)} \right)^{1/2} e^{\frac{i}{2\epsilon(z_f - z_i)}(x - x_i)^2}. \quad (5)$$

The kernel,  $K_f$ , for the focusing quadrupole magnet is given by

$$K_f(x_f, z_f; x_i, z_i) = \left( \frac{\sqrt{k_1}}{2\pi i \epsilon \sin(\sqrt{k_1}(z_f - z_i))} \right)^{1/2} e^{i \frac{\sqrt{k_1}}{2\epsilon} [(x_f^2 + x_i^2) \cot \sqrt{k_1}z - 2x_f x_i \csc \sqrt{k_1}z]}. \quad (6)$$

For the defocusing case the kernel is easily obtained by replacing the cot and csc functions in Eq.(6) with coth and csch functions, respectively.

Since the potential energy terms are related to linear forces, it is adequate enough to consider simple Gaussian integrations if the initial beam wave function is a Gaussian-type as follows,

$$\psi_1(x, 0) = \left( \frac{1}{2\pi\sigma_1^2} \right)^{\frac{1}{4}} \exp \left[ -\frac{x^2}{4\sigma_1^2} + i \left( \frac{x^2}{2\epsilon\rho_1} + \theta_1 \right) \right], \quad (7)$$

where  $\sigma_1, \rho_1, \theta_1$  are the initial values of the rms beam size, the curvature radius, and the input phase, respectively.

After the input beam passes through the linear optical elements, the beam wave function remains the same Gaussian function such as

$$\psi_2(x, z) = \left( \frac{1}{2\pi\sigma_2^2(z)} \right)^{\frac{1}{4}} \exp \left[ -\frac{x^2}{4\sigma_2^2(z)} + i \left( \frac{x^2}{2\epsilon\rho_2(z)} + \theta_1 + \theta_2(z) \right) \right]. \quad (8)$$

The different forms of the parameter functions,  $\theta_2, \sigma_2$ , and  $\rho_2$ , characterize the properties of each optical element.

In a drift space, the functions are given by

$$\sigma_2^2(z) = \sigma_1^2 \left[ \left( \frac{\epsilon z}{2\sigma_1^2} \right)^2 + \left( 1 + \frac{z}{\rho_1} \right)^2 \right], \quad (9)$$

$$\tan 2\theta_2(z) = -\frac{\epsilon}{2\sigma_1^2} \frac{z\rho_1}{z + \rho_1}, \quad (10)$$

$$\frac{1}{\rho_2(z)} = \frac{1}{\rho_1} \left[ \frac{\rho_1}{z} - \left( \frac{\sigma_1}{\sigma_2(z)} \right)^2 \left( 1 + \frac{\rho_1}{z} \right) \right]. \quad (11)$$

In a focusing quadrupole magnet, they are given by

$$\sigma_2^2(z) = \sigma_1^2 \left[ \left( \cos(\sqrt{k_1}z) + \frac{1}{\sqrt{k_1}\rho_1} \sin(\sqrt{k_1}z) \right)^2 + \left( \frac{\sigma_0}{\sigma_1} \right)^4 \sin^2(\sqrt{k_1}z) \right], \quad (12)$$

$$\tan 2\theta_2(z) = -\frac{\left( \frac{\sigma_0}{\sigma_1} \right)^2 \sin(\sqrt{k_1}z)}{\cos(\sqrt{k_1}z) + \frac{1}{\sqrt{k_1}\rho_1} \sin(\sqrt{k_1}z)}, \quad (13)$$

$$\frac{1}{\rho_2(z)} = \frac{1}{\rho_1} \left( \frac{\sigma_1}{\sigma_2(z)} \right)^2 \left[ \cos(2\sqrt{k_1}z) + \frac{1}{2} \left\{ \frac{1}{\sqrt{k_1}\rho_1} + \sqrt{k_1}\rho_1 \left( \left( \frac{\sigma_0}{\sigma_1} \right)^4 - 1 \right) \right\} \sin(2\sqrt{k_1}z) \right], \quad (14)$$

with  $\sigma_0^2 = \epsilon/(2\sqrt{k_1})$ . For a defocusing lens, the functions can be obtained by replacing  $\sqrt{k_1}$  for the focusing case with  $i\sqrt{k_1}$ . We can easily check to see if Eq. (8) is the solution of Eq. (1) by inserting the obtained beam wave function into the differential equation.

In order to check on the validity of the solutions, we compared them with the PARMILA simulation result with 50,000 macro particles through the FODO lattice. We selected a random distribution of the particles in the x-x' and y-y' spaces and neglected the space charge effects. The weighting function of the distribution is a Gaussian-type truncated at four times the standard deviation.

Since the particle distributions in the x' or y' spaces are not reflected in the initial curvature radius,  $\rho_1$ , we assumed a laminar distribution with constant divergences in the input beam. In the simulation, we selected  $1/\rho_1 \simeq 0$ , which means a large value of the twiss parameter,  $\beta$ , in both horizontal and vertical directions. We note that the input beam can be treated as a slice of an usual particle distribution in the transverse phase space.

The particle type is proton whose energy is 1 GeV in the calculation. The field gradient and effective length of the quadrupole magnets are 10 T/m and 0.4 m, respectively. The length of the drift space is 1 m. The properties of the input beam are summarized in Table 1.

Figure 1 shows the particle distributions of the input beam in both horizontal and vertical directions. The histograms are the PARMILA result with 50,000 macro particles. The real lines represent the Gaussian input beam of the model calculation. The input values of  $\sigma$  and  $\rho$  are obtained by using their relations to the twiss parameters,  $\alpha, \beta$ , and  $\gamma$ , and the emittance,  $\epsilon$ :  $\sigma^2 = \epsilon\beta$  and  $1/\rho = (1/\sigma)d\sigma/dz = -\alpha/\beta$  [5]. The numerical values of the input parameters in the model are given as

$$\begin{aligned} \sigma_1 &= 2.11 \text{ mm} & \rho_1 &= 282.38 \text{ m} & \text{for the horizontal direction,} \\ \sigma_1 &= 1.45 \text{ mm} & \rho_1 &= -253.09 \text{ m} & \text{for the vertical direction,} \\ k_1 &= 1.77 \text{ m}^{-2}, \end{aligned}$$

where  $k_1 = qG/(m\gamma_r\beta_rc)$  with the quadrupole field gradient,  $G$ .

Figure 2 and Figure 3 show the PARMILA simulations (histograms) and the model calculations (real-lines) in the horizontal and vertical directions, respectively. The lattice structure for the horizontal beam is FODO. It is DOFO for the vertical direction. We note that the thermal wave model describes the simulation result successfully in the transverse directions. In order to check the result quantitatively, we compared the rms beam sizes obtained by the model to the values by the best-fit of the PARMILA result. It is summarized in Table 2. It shows that the model results are the same to the simulation within 1 % level.

In conclusion, we used a functional method to solve the differential equation given in the thermal wave model which describes the transverse beam dynamics of the relativistic

particles. The main advantage of this functional method is that we can calculate the effects of each beam optical element separately. The information of each element is summarized in the kernel. The final beam wave function is easily obtained by the Gaussian integration of the product between the kernel and the initial Gaussian wave function. We found that there is a good agreement between the PARMILA simulation and the model calculation. Since the initial beam is limited to a laminar type in this work, the model should be extended to describe the usual particle distribution in the transverse phase spaces. Even though there is some limits to the application of this method, this functional method is a very efficient tool to study the transverse beam dynamics in the thermal wave model.

## ACKNOWLEDGEMENTS

This work is supported by the 21C Frontier R&D program in the Ministry of Science and Technology of the Korean government.

## References

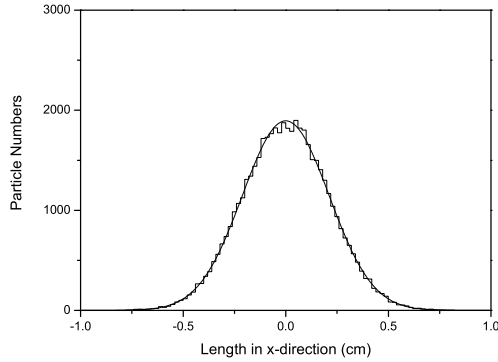
- [1] R. Fedele and G. Miele, *Nuovo Cimento D* 13 (1991) 1527.
- [2] R. Fedele and P. K. Shukla, *Phys. Rev. A* 45 (1992) 4045.
- [3] R. Fedele and G. Miele, *Phys. Rev. A* 46 (1992) 6634.
- [4] S. A. Khan and M. Pusterla, *Eur. Phys. J. A* 7 (2000) 583.
- [5] R. Fedele, F. Galluccio and G. Miele, *Phys. Lett. A* 185 (1994) 93.
- [6] R. Fedele, F. Galluccio, V. I. Man'ko and G. Miele, *Phys. Lett. A* 209 (1995) 263.
- [7] H. Holstein, *Topics in Advanced Quantum Mechanics* (Addison-Wesley, 1992).
- [8] H. Takeda and J. Billen, PARMILA, LA-UR-98-4478.

Table 1: The twiss parameters and emittances of the input beam in the transverse directions.

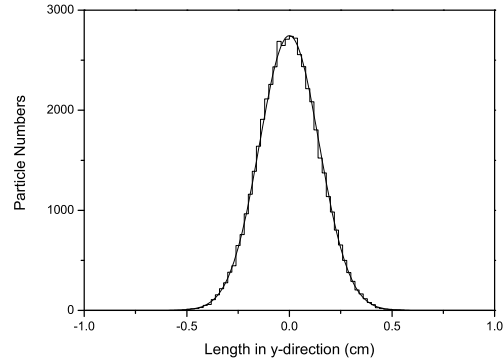
	$\alpha$	$\beta$ (m/rad)	$\epsilon$ ( $10^{-9}$ m-rad)
horizontal axis	-1.63	461.14	9.68
vertical axis	0.86	216.63	9.74

Table 2: The rms beam sizes obtained by the model and the best fit of the PARMILA result: the numbers in parentheses are the values in the vertical direction.

	model (mm)	simulation (mm)	difference (%)
After a F(D) lattice	1.825(1.661)	1.842(1.661)	-0.92(-)
After a drift space	0.406(2.729)	0.408(2.729)	-0.49(-)
After a D(F) lattice	0.130(2.760)	0.131(2.760)	-0.76(-)
After a drift space	1.452(1.842)	1.461(1.842)	-0.61(-)

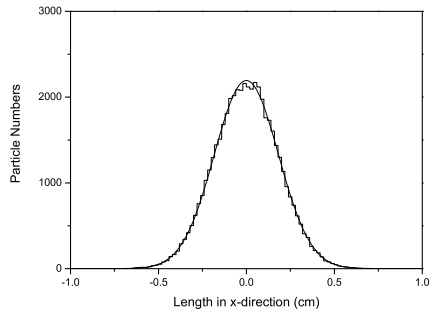


(a)

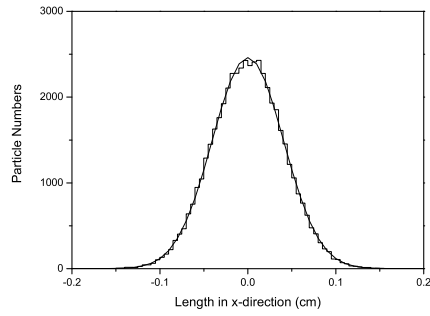


(b)

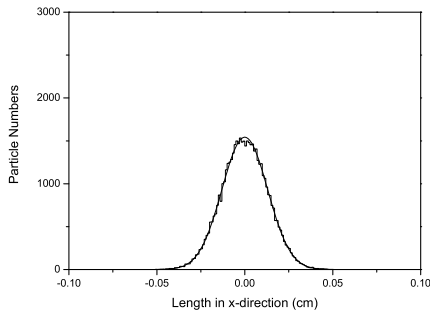
Figure 1: Particle distributions of the input beam in the horizontal (a) and vertical (b) directions. The histogram and real lines represent the PARMILA results and the model predictions, respectively.



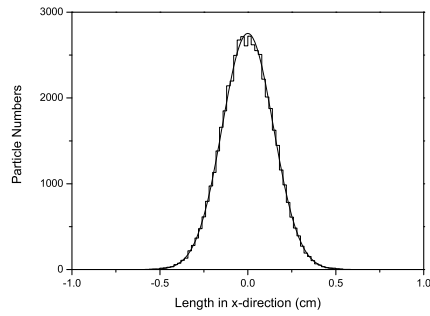
(a)



(b)



(c)



(d)

Figure 2: Particle distributions on the horizontal axis with histograms for the PARMILA results and real lines for the model calculations: (a) after a focusing quadrupole (b) after a drift space (c) after a defocusing quadrupole (d) after a drift space.

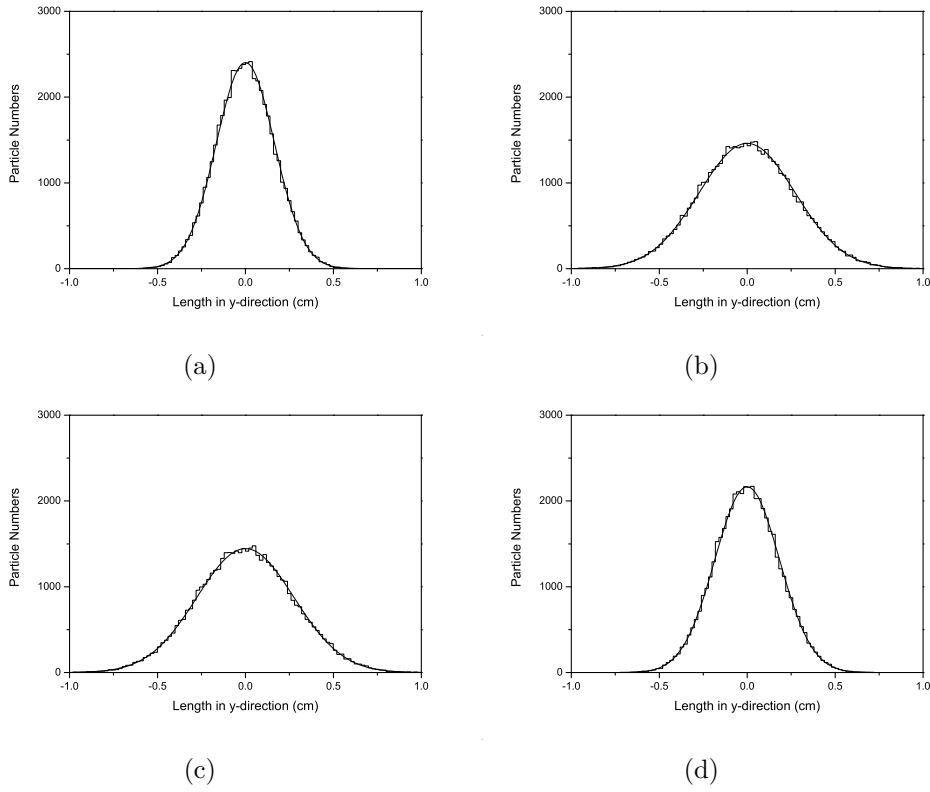


Figure 3: Particle distributions on the vertical axis with histograms for the PARMILA results and real lines for the model calculations: (a) after a defocusing quadrupole (b) after a drift space (c) after a focusing quadrupole (d) after a drift space.